ISBN-978-989-9121-19-5
BANGKOK 22nd International Conference on "Innovations in Engineering, Science & Technology" (BIEST-22)
Dec. 21-23, 2022 Bangkok (Thailand)

Experimental and Numerical Investigation of the Temperature Variation of the Single-Pass Solar Air Collector

Zar Chi Linn [1], War War Min Swe [1], Aye Aye Khaing [2] and Aung Kyaw Soe [1]

[1] Mechanical Engineering Department, Mandalay Technological University

[2] Mechanical Engineering Department, Technological University (Mandalay)

Mandalay, Myanmar

***Abstract*:** *This paper presents a study for thermal analysis that examines a flat plate solar air collector's experimental and numerical analysis. The temperature distribution of the single-pass flat plate solar air collector is analyzed in relation to various mass flow rates. The collector is tested in the courtyard of the Mechanical Engineering Department, Mandalay Technological University, Mandalay, Myanmar (latitude 21.98° N, longitude 96.1°E). In this paper, the solar air collector's heat flux is originally considered hourly for October 2022. The analysis is done with the numerical method (ANSYS) which is validated with respect to the experimental test. In the numerical result, the maximum output temperature is about 323K at the mass flow rate of 0.01935kgs^{-1}. This temperature is validated with the experimental result. The analysis's investigation revealed that the temperature variation of the solar air collector is reducing as mass flow rates increase.*

Keywords: *solar air collector, thermal analysis, mass flow rate, numerical analysis (CFD-CFX), experimental test*

1. Introduction

Solar air collectors are effective technologies according to their simplicity in industrial products, drying of timber, space heating, and food drying. They have a low-cost operation, are simple to maintain and design, and have green technology with no greenhouse gas emissions. Solar air collectors have only a few drawbacks: Low heat transfer coefficients cause solar air collectors to have low thermal efficiency.

Maytham Ali Jasim Al-Neama conducted to improve the thermal performance of the entire system, a thorough study of several solar collector designs combined with drying chambers will be carried out using heat transfer principles [2]. Mohammed Amine Amraoui presents to assess the flow and temperature distribution inside the solar collector using computational fluid dynamics (CFD) tool work that has been done both theoretically and experimentally [3]. A CFD investigation of heat transmission through inclined wavy solar collectors and flat-plate solar collectors was performed by Varol and Oztop [6]. They discovered that the geometry of the enclosure has an impact on fluid flow and heat transfer and enhances it when compared to a flat enclosure. A numerical simulation of a transpired solar air collector by Wang et al. revealed that the collector has important advantages in the ventilation preheating sector and also demonstrated that CFD techniques have their own benefits in the research of solar air collectors [8]. Ong forecasted the heat transfer properties of four different types of solar air heaters. On system efficiency, the effects of relevant parameters were discussed. According to his findings, a collector length of 1 m might be used to get satisfactory results [9]. Three different single-pass solar air heater models' performances were experimentally examined by Ong [10].

This study aims to assess the viability of setting up a higher-performance solar air collector in the Mandalay region of Myanmar. The simulations for the various collector output temperatures based on the varied mass flow rates are performed using ANSYS software. Different mass flow rates are used to compare the experimental and numerical temperature distributions. The design parameters of the solar air collector and its material will yield the desired effect to maximize its temperature.

2. System Description for Solar Air Collector

The solar air collector structure is fabricated using half-inch thick plywood material and is 1.2192 m long, 91.44 cm wide and 12 cm in height. To lessen convective heat loss to the environment, the absorber was mounted in a hardwood cabinet that was thermally insulated and covered with a glass plate with a 4 mm thickness. To maximize absorption and decrease solar radiation emissivity, the absorber which is made of aluminum was painted black. Due to the low temperature inside the collector, conduction through the insulation and convection caused by the wind is regarded to be insignificant collector thermal losses through the housing. The tilt angle of 45° is chosen because the value of solar insolation flux is maximum at this angle. The collector was put to the test outside. For detecting the air temperature and the temperature of the absorber plate, thermocouples are installed at the inlet, outlet, and center of the absorber plate. The wind speed was measured with a digital anemometer-type Lutron YK-2005. A Pyranometer is used to measure the heat flux caused by solar irradiation that is incident on the absorber plate. Every 10 minutes, the air temperature at the collector's inlet and outflow, the ambient temperature, the temperature of the absorber, and the wind speed were recorded. All examinations ran from 9:00 am to 4:00 pm. Under clear skies, experiments were carried out in October 2022. A schematic view of the experimental setup of the constructed solar air collector is shown in Fig. 1. In the present modeling, the data used are shown in Table I [1].

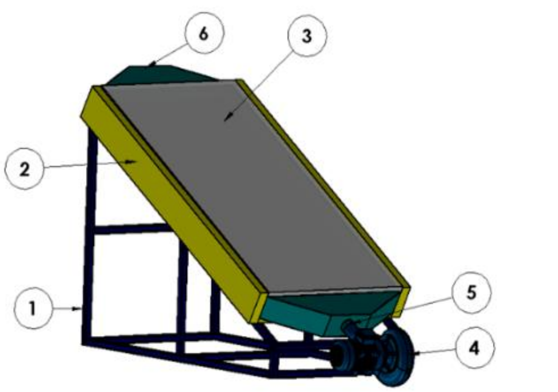

Fig. 1: Schematic diagram of solar air collector (1) collector stand, (2) insulation material, (3) glass cover, (4) air fan, (5) air inlet, (6) air outlet

TABLE I: Characteristics of solar air collector

No	Component	Material	Parameter	Specification	Unit
1	Transparent cover	Glass	Length Width Thickness	1.2192 0.9144 0.004	m
2	Absorber plate	Aluminum	Length Width Thickness	1.2192 0.9044 0.002	m
3	Insulator	Foam	Length Width Thickness	1.2192 0.9044 0.0127	m
4	Cover box	Plywood (floor)	Length Width Thickness	1.2192 0.9044 0.0127	m
		Plywood (side)	Length Width Thickness	1.2192 0.1083 0.0127	m
5	Air channel (cross-section)	Aluminum Wood	Length Width	0.9044 0.0886	m
6	Air duct	steel	Diameter	0.0762	m

3. Numerical Analysis

3.1 Geometry

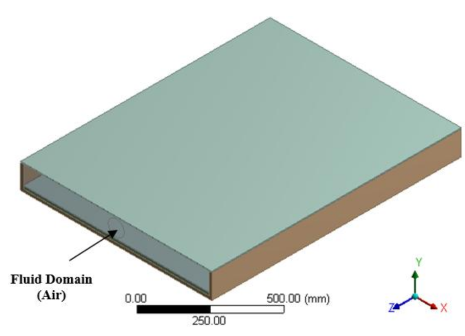

Fig.2: Extracted volume of single-pass solar air collector geometry

The fluid domain and solid domains are created for this analysis. The fluid domain is used for thermal flow between the glass and absorber. The working fluid is air at 25 ˚C for numerical analysis. The solid domains are glass, foam, and plywood. The configuration of a single-pass solar air collector is shown in fig.2.

3.2 Mesh

The mesh generates inside the volume and on suffuse of the fluid domain and solid domain. The physics preference of analysis is CFD-CFX. The maximum face size is 0.15m and the minimum size is 7.52e-004m. The number of an element is about a 2.3millon and the number of nodes is 1.7 million. Tetrahedron meshing is used for surface and volume meshing, and it is depicted in fig. 3.

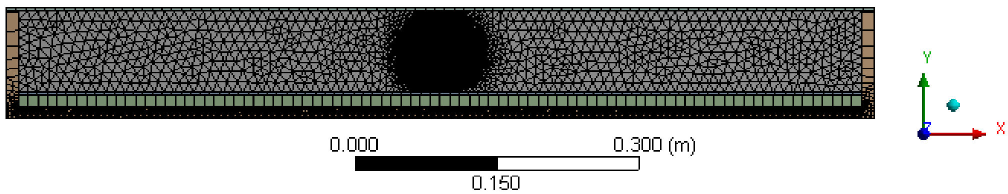

Fig. 3: A 3D mesh of Solar Flat Plate Collector

3.3 The boundary conditions

The setup boundary condition for the single air pass collector is listed in Table II. Air flows into the solar collector's intake before exiting through its outlet. The wall boundary is a plywood and foam adiabatic wall with no slide properties. These are heat transfers from the air domain to the glass. Thermal energy is the analytical type. The k-Epsilon turbulence model is used. The Prandtl Number for turbulent flow is 0.7202. Table II displays the physical and thermal characteristics of various engineering materials employed in the simulation

Table II: Thermal and fluid properties of the material used in a simulation study

Material	Density (kg/m^3)	Specific heat capacity (J/kgK)	Thermal conductivity (W/mK)
Air	1.059	1007	0.02808
Aluminium plate (Absorber)	2710	900	238
Glass (Cover)	2500	840	1.4
Foam (Insulation)	23	1131	0.035

4. Experimental Setup

An experimental setup was designed and tested at the Mandalay Technological University, Myanmar (latitude 21.98° N, longitude 96.1°E). The experiments were conducted for various air mass flow rates between 0.01935 kg/s and 0.038925 kg/s, the air being vehiculated by 12 V, 0.6 A fan. The fan is programmed and controlled on the Arduino board which controls the air mass flow rates. Fig. 4 depicts the solar air collector's planned layout. Fig.4 (a) shows the setup assembly and individual parts of the solar air collector. The temperature measuring point is described in Fig.4 (b). The temperature sensors are positioned at the solar collector's entry, in the middle of it, and at the collector's output. Fig.4 (c) displays the data obtained from these sensors. This temperature is a result of local measurements made during the hours of 9:00 am and 4:00 pm.

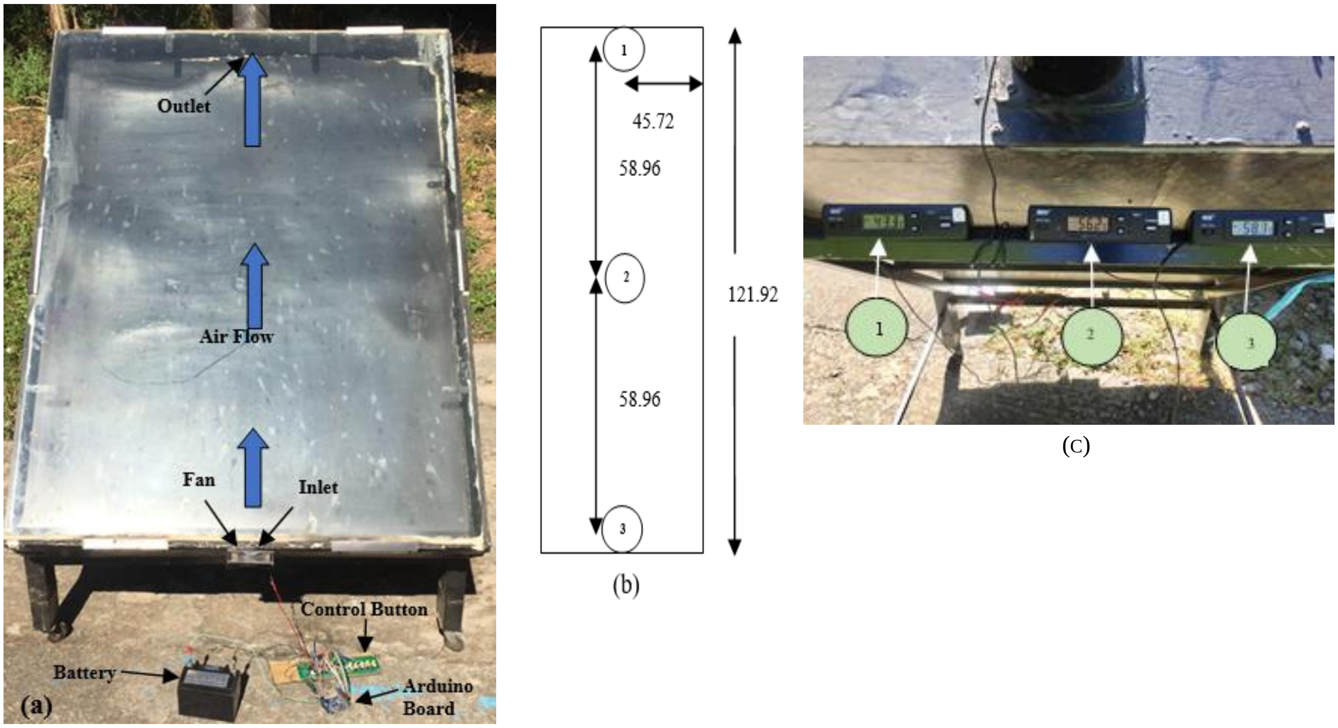

Fig.4: (a) Solar air collector (b) Locations of the thermocouples (Dimension are in cm) and (c) sensors

5. Results and Discussions

After conducting an experimental investigation of the collector, the numerical analysis is completed using the mass flow rates that were used in the experimental study as input. One of the crucial factors affecting a collector's performance is the mass flow rate of the air passing through it. In the numerical analysis, the generated model is used to calculate the exit temperature of air from the collector at various flow rates. The outlet temperatures and the change in mass flow rates were compared using numerical data and experimental data.

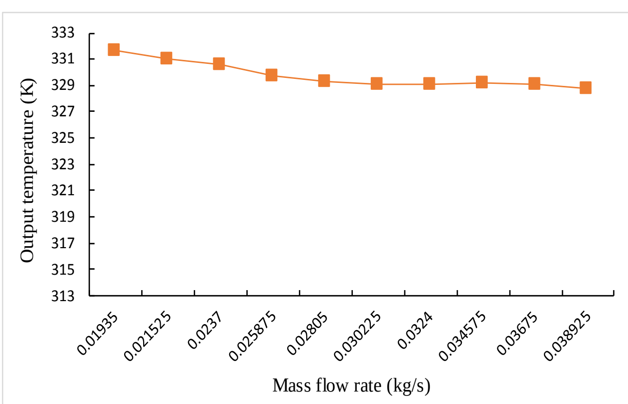

Fig. 5: Average output temperature (October 3, 2022)

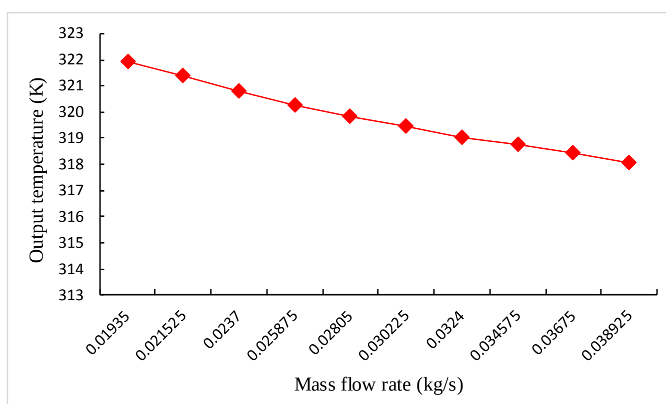

Fig. 6: Average output temperature (October 2022)

Fig. 5 represents the variation of the output temperature of the collector with the mass flow rates for October 3, 2022. As the flow rate rises, the air has less time to absorb solar heat, which affects the output temperature. Thus, the temperature has reverse relation with the flow rate which is also affirmed in Fig.5. Fig. 6 represents the variation of the outlet temperature with the various mass flow rates for the average temperature of the days of October 2022.

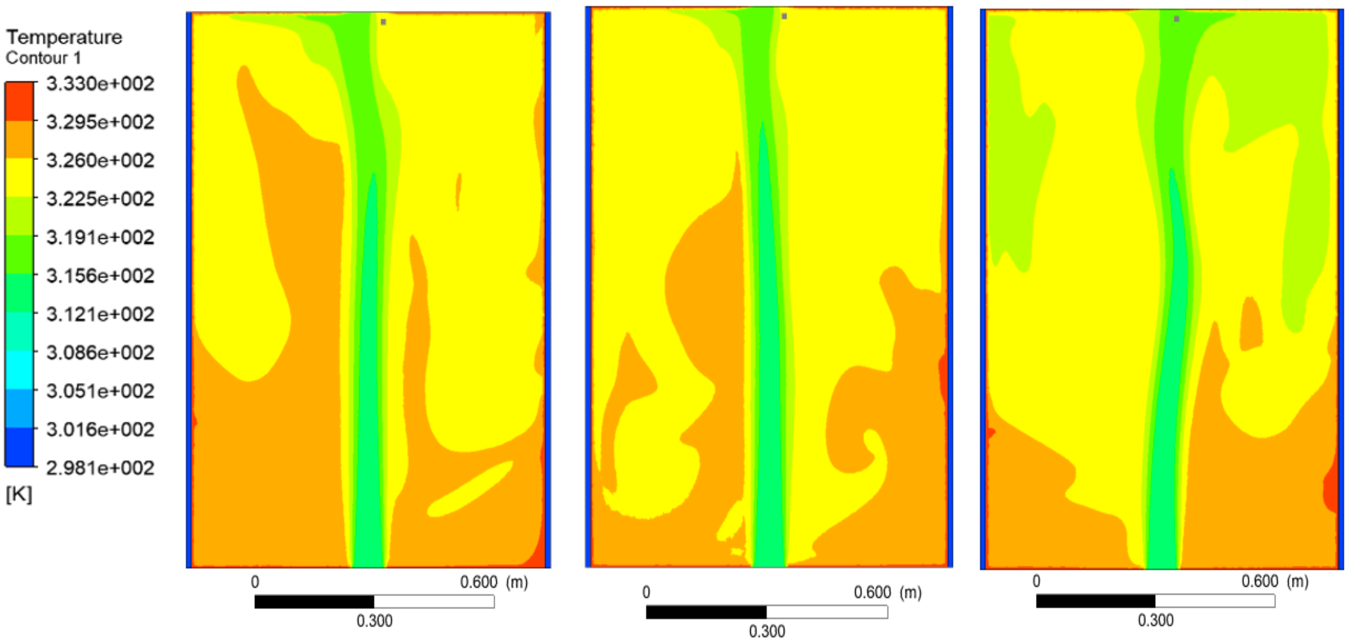

(a) (b) (c)

Fig.7(a): Output temperature corresponding to the mass flow rate of 0.01935kgs^{-1} (b) Output temperature corresponding to the mass flow rate of 0.02805 kgs^{-1} (c) Output temperature corresponding to the mass flow rate of 0.038925 kgs^{-1}

Figures, Fig.7(a), (b), and (c) show temperature contour plots of the air domain for each of the mass flow rates of 0.01935 kgs^{-1}, 0.02805 kgs^{-1}, and 0.038925 kgs^{-1}. This is the comparison with the temperature contour plot for the same coordinate. The output temperatures are measured with the probe at the same coordinate: x = -0.0372976, y = 0.0433358, z = 1.17331. In those figures, the temperature drops as the mass flow rate increases. To get the average temperature, five points were probed at the outlet of the collector for each airflow rate. Fig.8 describes that the average temperature of each mass flow rate decreases as the mass flow rates increase.

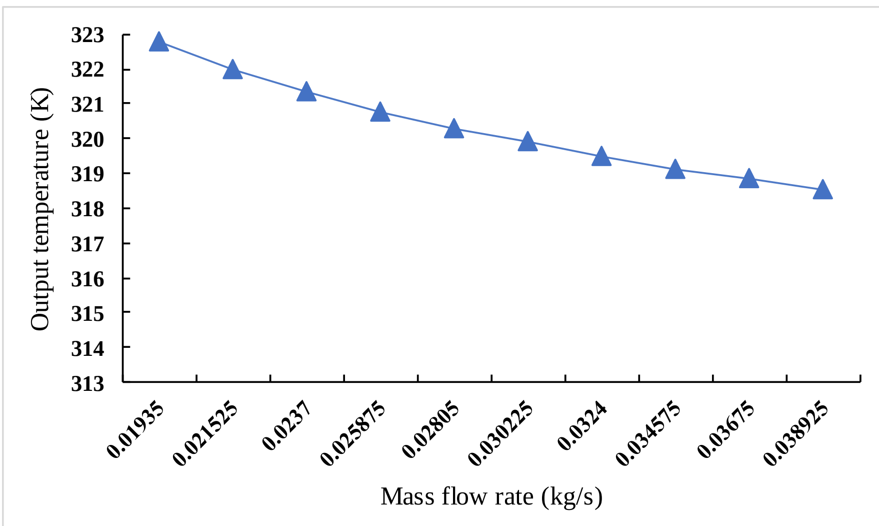

Fig.8: Variation of output temperature with mass flow rates

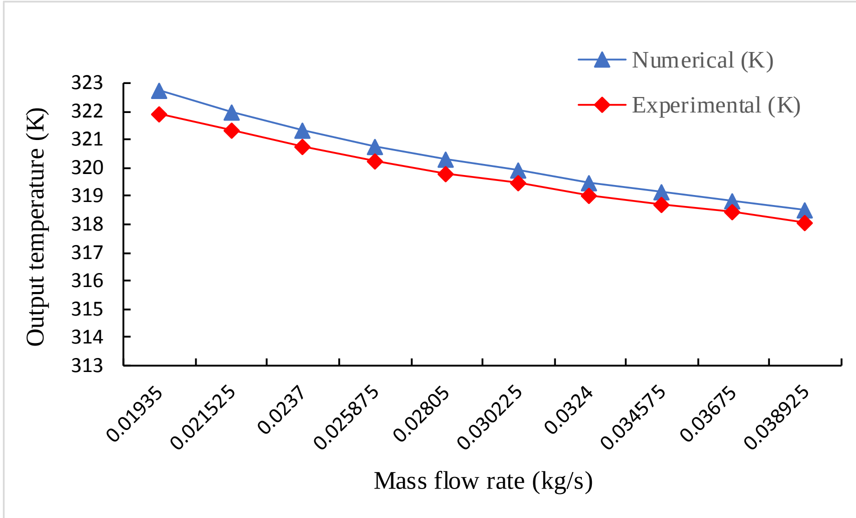

Fig.9: Comparison between experimental and simulated result values of outlet temperatures

Fig. 9 shows the validation plot for the temperature rise of the air corresponding to the ten mass flow rates for solar air collector by comparison between outlet air temperatures of the CFD simulation study and experimental study. Variation of readings is within acceptable limits. The simulation program showed that the outlet temperature is about 323K at the mass flow rate of 0.01935kg s^{-1} at solar insolation of 894.4 Wm^{-2} and ranged from mass flow rates of 0.01935 kg s^{-1} to 0.038925 kg s^{-1}, although the experimental results showed a collector output temperature of about 322K. Results obtained through simulation show good agreement with experimental results.

6. Acknowledgements

The author is in deep gratitude to Dr. San Yu Khaing, Pro-Rector, of Mandalay Technological University. The author would like to give particular appreciation to Dr. War War Min Swe, Professor, and Head of the Department of Mechanical Engineering, at Mandalay Technological University, for her invaluable supervision and guidance to complete this paper.

7. References

[1] John A. Duffie, William A. Beckman, "Solar Engineering of Thermal Processes," Fourth Edition, Solar Energy Laboratory, University of Wisconsin-Madison.pp.280-298

[2] Maytham Ali Jasim Al-Neama, "Performance Enhancement of Solar Air Collectors Applied for Drying Processes," Ph.D. thesis, Dept. Mechanical Eng., Szent István Univ., Gödöllő, Hungary, 2018.

[3] Mohammed Amine Amraoui, "Three-Dimensional Analysis of Air Flow in a Flat Plate Solar Collector," 62(2), pp. 126-135, 2018 https://doi.org/10.3311/PPme.11255, December 2017.

https://doi.org/10.3311/PPme.11255

[4] Faris Aissaoui, "Experimental and Theoretical Analysis on Thermal Performance of the Flat Plate Solar Air Collector," ISSN: 0392-8764, Vol. 34, No. 2, June 2016, Algeria.

https://doi.org/10.18280/ijht.340209

[5] M.A. Karim and Z.M. Amin, "Mathematical Modelling and Performance Analysis of Different Solar Air Collectors," IIUM Engineering Journal, Vol. 16, No. 2, 2015.

https://doi.org/10.31436/iiumej.v16i2.603

[6] Varol, Y. and Oztop, H.F., “A Comparative Numerical Study on Natural Convection in Inclined Wavy and Flat-Plate Solar Collectors”, Building and Environment, Volume 43, pp. 1535-1544, 2008.

https://doi.org/10.1016/j.buildenv.2007.09.002

[7] Selmi, M., Al-Khawaja, M.J., and Marafia, A., “Validation of CFD simulation for flat plate solar energy collector”, Renewable Energy, Volume 33, pp. 383-387, 2008.

https://doi.org/10.1016/j.renene.2007.02.003

[8] Wang, C., Guan, Z., Zhao, X., and Wang, D.,” Numerical Simulation Study on Transpired Solar Air Collector” Renewable Energy Resources and a Greener Future, Volume 8, pp 3-4, 2006.

[9] K. Ong, “Thermal performance of solar air heaters: mathematical model and solution procedure,” Solar Energy, vol. 55, pp. 93–109, 1995a. DOI: 10.1016/0038-092X(95)00021-I

https://doi.org/10.1016/0038-092X(95)00021-I

[10] K. Ong, “Thermal performance of solar air heaters: experimental correlation,” Solar Energy, vol. 55, pp. 209–220, 1995b. DOI: 10.1016/0038- 092X(95)00027O.

https://doi.org/10.1016/0038-092X(95)00027-O